Can Peripheral Representations Improve Clutter Metrics on Complex Scenes?

Arturo Deza
Dynamical Neuroscience
Institute for Collaborative Biotechnologies
UC Santa Barbara, CA, USA
deza@dyns.ucsb.edu

Miguel P. Eckstein
Psychological and Brain Sciences
Institute for Collaborative Biotechnologies
UC Santa Barbara, CA, USA
eckstein@psych.ucsb.edu

Supplementary Material

Beyond Foveated Feature Congestion

We extended other clutter models to their respective peripheral versions. Since the other models: Edge Density, Subband Entropy and ProtoObject Segmentation have not been designed to produce an intermediate step with a dense clutter pixel-wise representation (unlike Feature Congestion), it is hard to find respective optimal dense clutter representations without losing the essence of each model. For Edge Density, we compute the magnitude of the image gradient after grayscale conversion. For Subband Entropy, we decided to keep all the respective subbands, as the model proposes as well as the coefficients that are used to compute a weighted sum over the entropies. In other words, our dense version of Subband Entropy is more of a dense "Subband Energy" term, since computing Entropy over a vector of a small $N \times K$ vector space of $N = 3$ scales and $K = 4$ orientations produced very little room for variation. Finally dense ProtoObject Segmentation was computed by following the intuition of final number of superpixels over inital number of superpixels, but since this is not applicable at a pixel wise level, we decided to compute multiple ProtoObject Segmentations with different regularizer and superpixel radius parameters, and averaged all superpixel segmentation ratios – where every map was dense at a superpixel level, and each superpixel score was the initial number of pixels over the final number of initial number of pixels that belong to that superpixel after the meanshift merging stage in HSV color space.

Foveated Feature Congestion *vs* Hit Rate correlation					
Distance	4 deg	6 deg	8 deg	10 deg	12 deg
L1-norm	-0.80 ± 0.04	$\mathbf{-0.82 \pm 0.04}$	-0.81 ± 0.05	-0.79 ± 0.05	-0.76 ± 0.06
L2-norm	$\mathbf{-0.79 \pm 0.05}$	$\mathbf{-0.79 \pm 0.06}$	-0.77 ± 0.06	-0.75 ± 0.07	-0.71 ± 0.07
KL-divergence	-0.80 ± 0.04	$\mathbf{-0.82 \pm 0.04}$	$\mathbf{-0.82 \pm 0.04}$	-0.81 ± 0.05	-0.77 ± 0.06

Foveated Edge Density *vs* Hit Rate correlation					
Distance	4 deg	6 deg	8 deg	10 deg	12 deg
L1-norm	$\mathbf{-0.76 \pm 0.06}$	-0.73 ± 0.07	-0.69 ± 0.08	-0.65 ± 0.09	-0.59 ± 0.09
L2-norm	$\mathbf{-0.72 \pm 0.07}$	-0.66 ± 0.08	-0.62 ± 0.09	-0.56 ± 0.10	-0.50 ± 0.11
KL-divergence	$\mathbf{-0.76 \pm 0.06}$	$\mathbf{-0.76 \pm 0.06}$	-0.73 ± 0.07	-0.69 ± 0.08	-0.63 ± 0.08

Foveated Subband Entropy *vs* Hit Rate correlation					
Distance	4 deg	6 deg	8 deg	10 deg	12 deg
L1-norm	-0.75 ± 0.04	$\mathbf{-0.77 \pm 0.04}$	$\mathbf{-0.77 \pm 0.05}$	-0.76 ± 0.05	-0.73 ± 0.06
L2-norm	-0.74 ± 0.05	$\mathbf{-0.76 \pm 0.05}$	$\mathbf{-0.76 \pm 0.05}$	-0.75 ± 0.06	-0.71 ± 0.06
KL-divergence	-0.79 ± 0.04	-0.83 ± 0.04	$\mathbf{-0.84 \pm 0.04}$	-0.83 ± 0.04	-0.80 ± 0.05

Foveated ProtoObject Segmentation *vs* Hit Rate correlation					
Distance	4 deg	6 deg	8 deg	10 deg	12 deg
L1-norm	-0.70 ± 0.06	$\mathbf{-0.74 \pm 0.06}$	$\mathbf{-0.74 \pm 0.06}$	-0.72 ± 0.06	-0.66 ± 0.07
L2-norm	-0.74 ± 0.04	$\mathbf{-0.76 \pm 0.05}$	$\mathbf{-0.76 \pm 0.05}$	-0.76 ± 0.06	-0.72 ± 0.06
KL-divergence	-0.66 ± 0.06	$\mathbf{-0.71 \pm 0.05}$	-0.68 ± 0.06	-0.61 ± 0.07	-0.54 ± 0.08

Table 1: Foveated Clutter Models distance and ROI window length (deg) search.

29th Conference on Neural Information Processing Systems (NIPS 2016), Barcelona, Spain.

PIFC maps

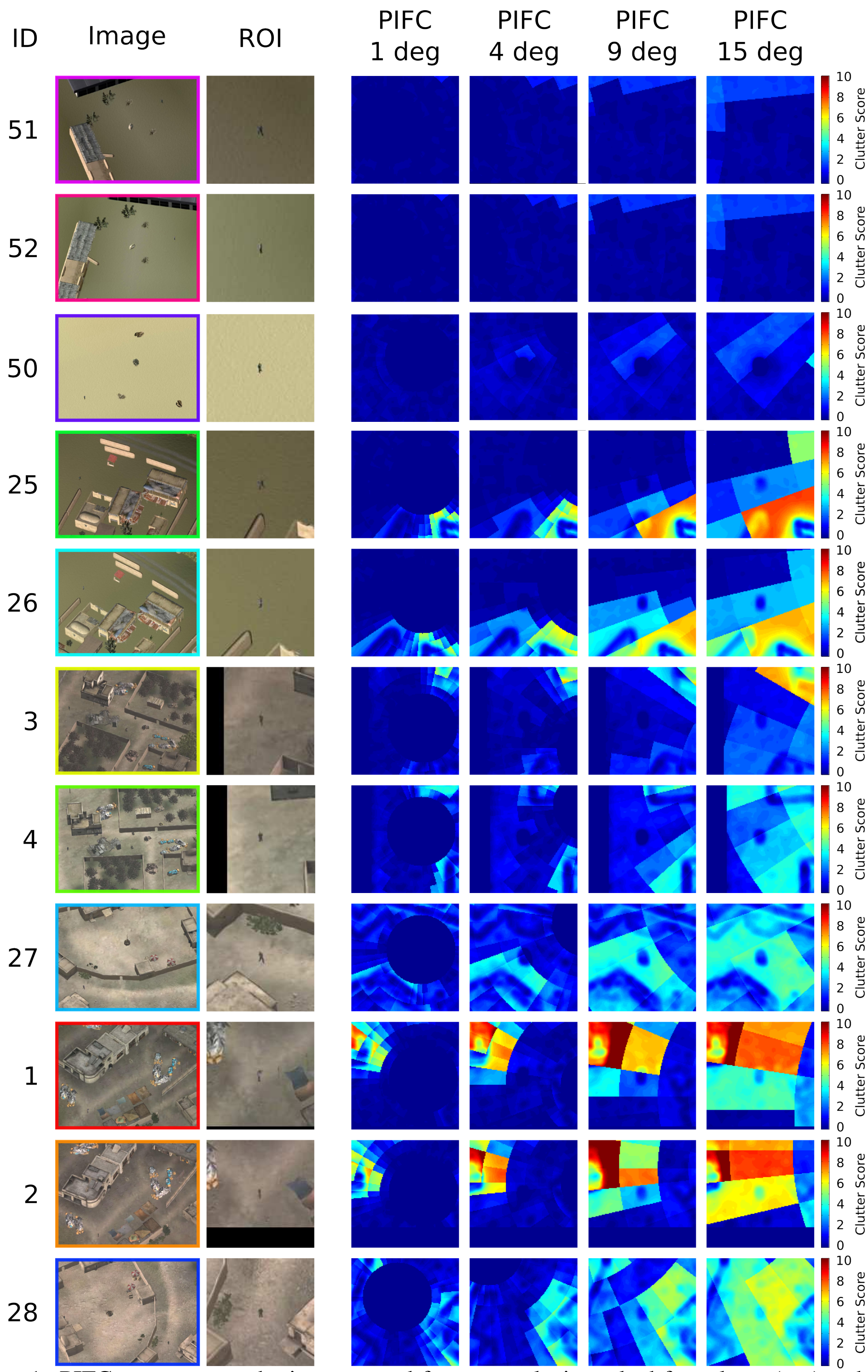

Figure 1: PIFC maps across the images used for our analysis ranked from least (top) to highest (bottom) FFC clutter as shown in Fig.6. Notice how the clutter scores (heatmap values) in the PIFC increase as a function of eccentricity and is contingent on the amount of clutter in the ROI.